Journal of Hazardous Materials 168 (2009) 145–155

Contents lists available at ScienceDirect

Journal of Hazardous Materials

journal homepage: www.elsevier.com/locate/jhazmat

A means to estimate thermal and kinetic parameters of coal dust layer from hot surface ignition tests

Haejun Park, Ali S. Rangwala*, Nicholas A. Dembsey

Department of Fire Protection Engineering, Worcester Polytechnic Institute, 100 Institute Road, Worcester, MA 01609, United States

ARTICLE INFO

Article history:
Received 9 July 2008
Received in revised form 31 January 2009
Accepted 3 February 2009
Available online 12 February 2009

Keywords:
Coal dust
Hot-surface
Ignition
Property estimation
Spontaneous combustion

ABSTRACT

A method to estimate thermal and kinetic parameters of Pittsburgh seam coal subject to thermal runaway is presented using the standard ASTM E 2021 hot surface ignition test apparatus. Parameters include thermal conductivity (k), activation energy (E), coupled term (QA) of heat of reaction (Q) and pre-exponential factor (A) which are required, but rarely known input values to determine the thermal runaway propensity of a dust material. Four different dust layer thicknesses: 6.4, 12.7, 19.1 and 25.4 mm, are tested, and among them, a single steady state dust layer temperature profile of 12.7 mm thick dust layer is used to estimate k, E and QA. k is calculated by equating heat flux from the hot surface layer and heat loss rate on the boundary assuming negligible heat generation in the coal dust layer at a low hot surface temperature. E and QA are calculated by optimizing a numerically estimated steady state dust layer temperature distribution to the experimentally obtained temperature profile of a 12.7 mm thick dust layer. Two unknowns, E and QA, are reduced to one from the correlation of E and QA obtained at criticality of thermal runaway. The estimated k is 0.1 W/m K matching the previously reported value. E ranges from 61.7 to 83.1 kJ/mol, and the corresponding QA ranges from 1.7×10^9 to 4.8×10^{11} J/kg s. The mean values of E (72.4 kJ/mol) and QA (2.8×10^{10} J/kg s) are used to predict the critical hot surface temperatures for other thicknesses, and good agreement is observed between measured and experimental values. Also, the estimated E and QA ranges match the corresponding ranges calculated from the multiple tests method and values reported in previous research.

1. Introduction

Thermal runaway, also described as supercritical self-heating or spontaneous ignition, has been considered as a serious hazard in many industrial processes and applications such as bulk coal stockpiles [1–3], nickel–cadmium accumulators [4], and dust material deposits on a heated surface [5]. Ignition in dust deposits by thermal runaway can also lead to subsequent dust explosions [6].

Various methods and techniques have been developed to evaluate the propensity of thermal runaway of a material: hot plate test, oven-basket test, thermal analysis test, etc. [7]. Since thermal runaway can occur in various circumstances, each test method has its own merits in application. The hot plate test is specifically designed to evaluate the thermal runaway hazard of a granular material up to a couple of centimeters, a realistic thickness in many industrial environments. The bottom surface of the dust layer is exposed to a hot plate while the top surface is cooled in ambient air. Despite being a relatively short and easy test procedure and resembling actual hazardous conditions closer than the other test methods in terms of sample amount and configuration, hot plate test has been considered just an approximate screening method on the basis of 'go/no go' criteria [8,9]. The oven-basket test, historically the most common test method, represents thermal runaway of granular materials surrounded by constant temperature. This method requires a wire mesh basket, usually cubical in shape, which contains the test material to be placed in an oven at a high temperature. Due to small sample dimensions compared to a real storage size, a high oven temperature is required to cause thermal runaway. The test results are then extrapolated to assess the hazard of a realistic storage stockpile. A review of the oven test and its application to a realistic scenario is given by Jones [10,11]. Thermal analysis tests such as thermogravimetric analysis (TGA) and differential scanning calorimetry (DSC) can measure the critical decomposition temperatures and heat energy produced by the chemical reactions. In these two tests, heat transfer phenomena are of less concern relative to chemical reaction [12] due to a tiny amount of test sample.

Parameters required for determining the thermal runaway hazard of a dust material including thermal conductivity, total heat transfer coefficient, activation energy, and pre-exponential factor in an Arrhenius equation are rarely known or are test environment

* Corresponding author. Tel.: +1 858 344 1946.
E-mail address: rangwala@wpi.edu (A.S. Rangwala).

0304-3894/$ – see front matter © 2009 Elsevier B.V. All rights reserved.
doi:10.1016/j.jhazmat.2009.02.010

specific. Some of these values can be obtained from other test methods such as TGA and DSC, and multiple hot plate tests with different dust layer thicknesses. The objectives of this study are to estimate these parameters from the hot plate test with a single thickness as compared to the multiple tests method by optimizing a numerical solution to match the experimental temperature distribution in the dust layer. Pittsburgh seam coal dust, one of the benchmark test materials of ASTM E 2021 [13], is used as the test material.

2. Background

The thermal runaway theory by Semenov [14] assumes constant temperature distribution throughout a reaction zone with heat loss at the boundary. However, Semenov's theory is only applicable to cases such as a well-stirred gas mixture due to the assumption of no thermal resistance in the reaction zone. Frank-Kamenetskii [15] adopted temperature distribution in the reaction zone, but assumed no heat loss on the boundary. Limitations of each of these cases were overcome by Thomas and Bowes [18] taking into account temperature distribution both in a reaction zone and heat loss on the boundaries [16].

Thermal runaway implies a sudden temperature increase due to thermal imbalance between heat generation rate and loss rate. Heat generation rate is known to follow the Arrhenius equation as an exponential function of temperature, and heat loss rate can be represented as a linear function of temperature as shown in Fig. 1(A). For an asymmetrically heated dust layer, heat transferred from the hot surface increases the dust layer temperature and consequently leads to a higher heat generation rate. Heat generated by exothermic reaction at the elevated temperature in the layer competes with the heat loss by convection and radiation at the top surface. Therefore, for a given material, layer thickness, and ambient environment, the hot surface temperature is the variable which determines the occurrence of either a thermal balance or thermal runaway. In Fig. 1(A), if the hot plate temperature (T_p) is set and remains at T_{p3} where heat generation rate in the dust layer is equal to the loss rate at the boundary, dust layer temperature will remain in steady state. However, any slight increase of heat generation rate can lead to thermal runaway. If T_p is set and remains lower than T_{p3} such as at T_{p2} where heat generation rate in the dust layer is higher than heat loss rate, the dust layer temperature will increase up to the point A where a thermal balance exists. A perturbation can cause temperature to increase beyond the point A, but the higher heat loss rate between T_{p2} and T_{p3} will direct it back to the steady state point A. Another thermal balance point C can be seen to be unstable since below point C heat loss rate is higher than heat generation rate, which yields temperature drop, and above point C thermal runaway occurs. In case of heating process with starting temperature lower than T_{p3}, point A is the only thermal balance point. As hot surface temperature increases from T_{p2} to T_{p3}, point C decreases and merges with point A resulting in point B. If T_p is set and remains at T_{p4} which is just above T_{p3}, dust layer temperature continuously increases and reaches thermal runaway.

Presumed temperature distributions in an asymmetrically heated dust layer with thickness $2r$ are shown in Fig. 1(B). A dust layer comes into contact with a hot surface at $x = 0$. Line 1 represents linear temperature distribution of an inert material without internal heat generation. The slope is determined by the heat loss rate on the top boundary at $x = 2r$ and thermal conductivity with a given T_p at T_{p1}. Curve 2 represents steady state condition at a low hot plate temperature with relatively small amount of heat generation in the dust layer. Curve 3 represents the maximum steady state condition of a dust layer. The maximum layer temperature (T_m) is observed at x_m very close to the hot surface. Curve 4 represents a transient temperature profile of thermal runaway. Higher oxygen concentration near the open boundary causes more reaction, and consequently, higher temperature than the lower area of the dust layer. The layer ignition temperature (LIT) or the minimum hot plate temperature for thermal runaway exists at T_{p4}. This is the main concern in most cases, and can be derived from the analytical solution of T_{p3}, since thermal runaway is theoretically expected to occur just above T_{p3}.

The analytical solution for T_{p3}, the maximum hot plate temperature for the dust layer to remain in steady state, is available from Thomas's thermal runaway model [17] with the assumption of negligible reactant depletion [18,19]. Assuming the dust layer as an infinite slab, a one dimensional steady state heat conduction equation can be written as,

$$k\frac{\partial^2 T}{\partial x^2} = -\rho Q A e^{-E/RT}, \tag{1}$$

where k = thermal conductivity of dust layer (W/m K), T = temperature (K), ρ = density (kg/m^3), Q = heat of reaction (J/kg), and A = Arrhenius pre-exponential factor (1/s). Q and A can be treated as one combined term (QA) for mathematical convenience. In the exponential part, E = the activation energy (J/mol) and R = the universal gas constant (=8.314 J/mol K).

Boundary conditions of constant temperature at the bottom surface and Newtonian cooling on the top surface are,

$$T = T_p \quad \text{at } x = 0, \tag{2a}$$

$$-k\frac{dT}{dx} = h_t(T_s - T_a) \quad \text{at } x = 2r, \tag{2b}$$

where $h_t = h_c + h_r$ = total heat transfer coefficient (W/m^2 K) accounting for convective (h_c) and radiant (h_r) heat transfer. T_s = top surface temperature (K), T_a = ambient temperature (K).

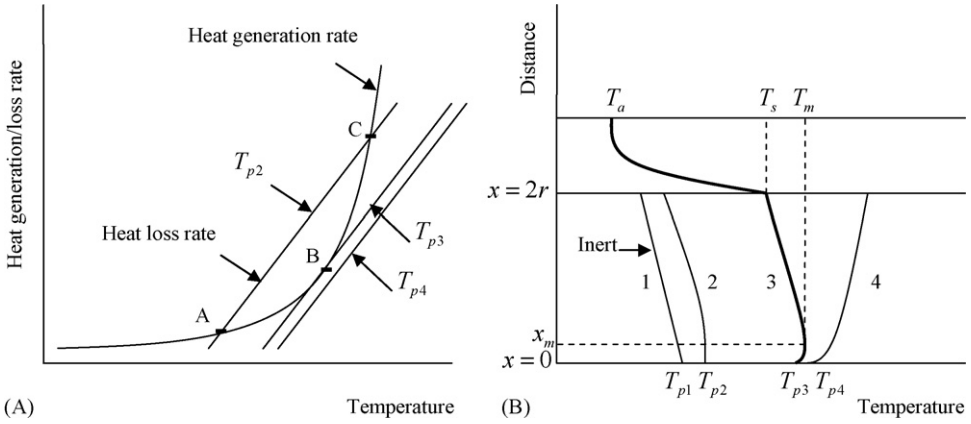

Fig. 1. Thermal runaway concept (A) and temperature distributions in asymmetrically heated dust layer (B).

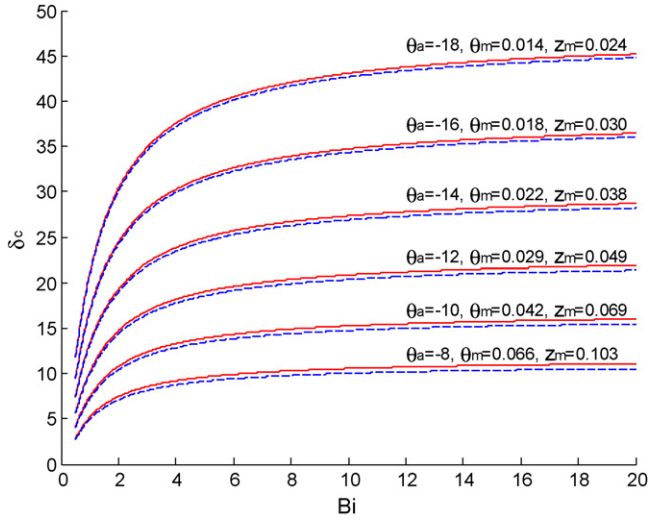

Fig. 2. δ_c as a function of Bi, θ_a, θ_m, and z_m (solid lines) and approximate δ_c as a function of corresponding θ_a only (dotted lines) for asymmetrically heated slab. The values of z_m and θ_m are selected from Bowes [17].

Eq. (1) can be simplified by non-dimensionalizing the terms for a steady state condition.

$$\frac{\partial^2\theta}{\partial z^2} = -\delta e^{\theta}, \tag{3a}$$

where

$$\theta = \frac{E}{RT_p^2}(T - T_p) \tag{3b}$$

and

$$\delta = \frac{E}{RT_p^2}\frac{r^2\rho QA}{k}e^{(-E/RT_p)}, \tag{3c}$$

θ, $z = x/r$, and δ are dimensionless parameters for temperature, distance from a hot surface, and heat generation rate term, respectively. r = Half of the dust layer thickness (m).

Boundary conditions in Eq. (2a) and (2b) become,

$$\theta = 0 \quad \text{at } z = 0, \tag{4a}$$

$$-\frac{d\theta}{dz} = Bi(\theta_s - \theta_a) \quad \text{at } z = 2, \tag{4b}$$

where $Bi = h_t r/k$ = Biot number.

The non-dimensional maximum heat generation rate for steady state condition, δ_c, represented by curve 3 in Fig. 1(B) can be calculated as a function of Bi, θ_a, θ_m, and z_m substituting T_p with T_{p3}. Exact solution of δ_c is shown in Fig. 2 as solid lines. The values of z_m and θ_m in Fig. 2 are chosen from Bowes [17].

θ_m and z_m are the maximum layer temperature and its location in the dust layer. Since the maximum temperature in the dust layer occurs almost at the hot surface which yields another boundary condition, $d\theta/dz = 0$ at $z = 0$, δ_c can be approximated without z_m and subsequent θ_m terms. The approximate solution for δ_c becomes,

$$\delta_c \approx \frac{1}{2}\left(\frac{Bi}{1+2Bi}\right)^2(1.4 - \theta_a)^2. \tag{5}$$

Fig. 2 shows the approximate solution as dotted lines.

Fig. 2 or Eq. (5) is used to determine whether thermal runaway is expected to occur for a given material. δ_c obtained from Fig. 2 or Eq. (5) is compared to δ calculated from Eq. (3c). δ_c requires Bi and θ_a. Bi can be calculated if thermal conductivity (k), total heat transfer coefficient (h_t) are available, and the dust layer thickness ($2r$) is measurable. Then, given a hot plate temperature (T_p), θ_a is calculated with activation energy (E) and ambient temperature (T_a). δ is calculated from Eq. (3c). In addition to the parameter values used for δ_c calculation, coupled pre-exponential term (QA) is required for Eq. (3c). If the condition, $\delta < \delta_c$ holds, the material is safe from a thermal runaway hazard. In this comparison procedure, k, E, and QA are required input in addition to the measurable dust layer thickness, density, and environment specific total heat transfer coefficient.

For Pittsburgh seam coal, these parameter values can vary with the test method, concerned temperature range, coal type, etc. Even for a given coal from the same mine field, variations exist in thermal properties [20]. Previous studies of thermal and kinetic parameters of Pittsburgh seam coal are shown in Table 1.

3. Experiments

Hot surface ignition tests of Pittsburgh seam coal dust layer with four different thicknesses: 6.4, 12.7, 19.1, and 25.4 mm, have been conducted. Two thermocouples for 6.4 mm and three thermocouples for the rest of the thicknesses were positioned at different heights in each dust layer to measure the temperature profile in the dust. Air flow in the test environment has been known to affect the LIT [29], current test results are from a quiescent environment with average air velocity of less than 0.01 m/s measured for half an hour and with ambient temperature (T_a) at 22 °C. Test results from 12.7 mm thickness were used to provide base line data for numerical calculation to estimate thermal conductivity and kinetic parameter values. The values of kinetic parameters obtained from a single 12.7 mm thick dust layer were then used to predict critical hot surface temperatures (T_{p3}) for the other layer thicknesses. Predicted T_{p3} were compared to the expected range of T_{p3} from the experiment. Test results from the other thicknesses were also used for the estimation of E and QA from the multiple tests method. Details about the multiple tests method are included in Appendix A.

3.1. Experimental set-up

The fundamental set-up and procedures of the dust layer test are similar to the ASTM E 2021[13] and Mirron and Lazzara's tests [8]. The basic test arrangement is shown in Fig. 3.

A circular aluminum disc (A) 25.4 mm in thickness and 203 mm in diameter was used as the hot surface. Disc A was thoroughly attached to the electrically heated plate (F), ROPH-144, Omega

Table 1
Properties of Pittsburgh seam coal.

Investigators	E (kJ/mol)	Q (J/kg)	A (1/s)	k (W/m K)	ρ (kg/m^3)	Technique
Howard and Essenhigh [21]	115.9		4.92×10^4			Flame furnace
Stone et al. [22]	102~114		1.1×10^5, ~5.41×10^6			Fluidized bed
Anthony et al. [23]	49.4		706			Electric grid
Kobayashi et al. [24]	104.6		6.6×10^4			Entrained flow
Yuan and Smith [25]	89.9		6×10^4	0.2	1300	
Singer and Tye [26]				0.19–0.21	1060–1297	Comparative slab
Herrin and Deming [27]				0.27	1340–1370	Cell technique
Reddy et al. [28]	65.4	$QA = 3.04 \times 10^9$		0.1	492	Hot plate

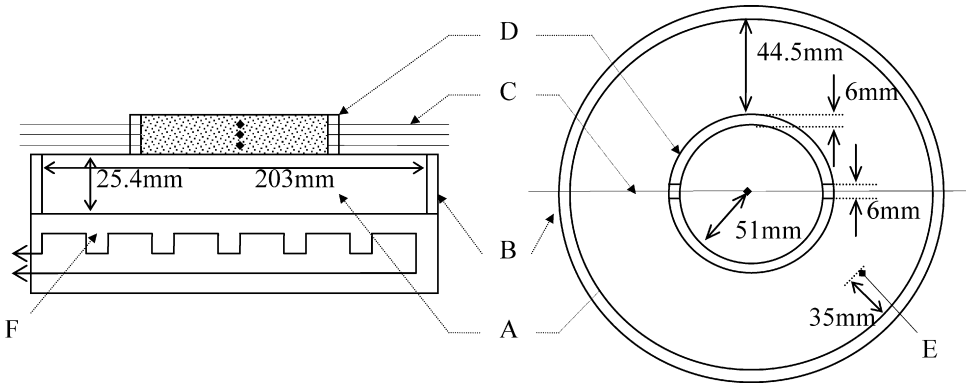

Fig. 3. Test apparatus arrangement for hot surface dust layer test: cross-sectional and top view with aluminum plate (A), insulation (B), dust layer thermocouples (C), steel ring (D), hot surface thermocouple (E) and hot plate (F) connected to power supply.

engineering, with thermally conductive cement, Omegabond 700, Omega engineering, to provide uniform temperature distribution on the aluminum plate surface. The perimeter wall was also wrapped by a 5 mm thick insulating material (B), ceramic paper 390, Cotronic Co., to minimize the heat loss to the environment. Hot surface temperature was measured by a Type K surface temperature thermocouple (E), CO1-K, Omega engineering, 35 mm inside from the plate edge. Thermal contact between the thermocouple and the hot surface was maintained by a metal clip attached to the plate frame. A temperature controller, CN 8592, Omega engineering, and solid state relay, SSRL240DC25, Omega engineering, were used to control and maintain the hot surface temperature at a steady value throughout any given test. Three stainless steel rings (D) of 102 mm ID, 114 mm OD: 6.4, 12.7 and 25.4 mm in height, respectively, were used to contain the dust layer. Two slots were located at diametrically opposite points on the rim to accommodate thermocouple wires. Type-K, bare thermocouples (C) with bead size of 0.38 mm OD, Omega engineering, were placed throughout the dust layer. Locations of the thermocouples varied with the thickness of the ring, i.e. the thickness of the dust layer. Thermocouples were positioned at 2 and 4 mm in height from the hot surface for 6.4 mm thick ring; 4, 7 and 10 mm for 12.7 mm thick ring; 3, 11, and 16 mm for 19.1 mm thick ring; 6, 12, 18 mm for 25.4 mm thick ring. The 19.1 mm thick ring was made up by stacking the 12.7 mm thick ring on top of the 6.4 mm thick ring. Temperatures of the dust layer were measured and recorded by National Instrument data acquisition system with an additional temperature recording device, HH506RA, Omega engineering, to confirm the temperatures.

Temperatures on the hot aluminum plate set at 250 °C showed very good uniformity. Temperatures were measured at 12 points on the hot surface, uniformly spaced, 6 points each and on two lines normal to each other. Except one point at which temperature was 249 °C, the other 11 points reported 250 °C. The thermocouples for both surface and dust layer temperature have an error of ±1.1 °C and the temperature controller, CN8592, has an error range of ±1 °C prescribed by the manufacturer. NI data acquisition unit has shown ±1 °C temperature fluctuation throughout tests. The inherent uncertainty of test apparatus is within an acceptable range since tests were conducted with either 5 or 10 °C resolution with respect to the layer ignition temperature.

Pittsburgh seam coal dust was provided by NIOSH Pittsburgh research laboratory. Its particle distribution with $D_{50,vol}$ of 48 μm is shown in Fig. 4 as reported by NIOSH. The measured average bulk density was 532 kg/m^3.

3.2. Experimental procedure

The steel ring was positioned in the center of the aluminum plate and adjusted to fit the slots with thermocouple wires. Bare thermocouples were located at the desired heights through the slots. Since direct contact of thermocouple wire to any metal may result in unstable and inexact temperature reading, the thermocouples were separated from the slots' surface by locating a piece of Cotronics' insulating material between them. After the thermocouples were positioned, the hot plate was turned on, and the desired temperature was set in the temperature controller. Once the hot plate temperature was stabilized, the steel ring was gently filled with a pre-measured amount of coal dust. The surface of the layer was evenly leveled with a flat iron ruler, and coal dust on the aluminum plate was removed. This procedure was carried out carefully so that the location of thermocouples in the dust layer was not disturbed. Tests were run until either the layer temperature reached a steady state for no less than 30 min or clear thermal runaway was observed. If thermal runaway did not occur at the pre-set hot plate temperature (T_p), it was increased by 10 °C until thermal runaway was observed. Resolution of 5 °C was adopted for 12.7 mm thick dust layer, the main data provider for numerical estimation, to reduce the error attributed to the test resolution. Fresh coal samples were used for each test.

3.3. Experimental results

Temperatures at 4, 7, and 10 mm heights of 12.7 mm thick layer are shown in Fig. 5(A) for both with and without thermal runaway at hot plate temperatures of 215 and 210 °C. Temperature profiles in the dust layer at specific times: 500, 2000, 2500, 3250 and 3750 s, in Fig. 5(B) are connected to Fig. 5(A) and referred to as a, b, c, d,

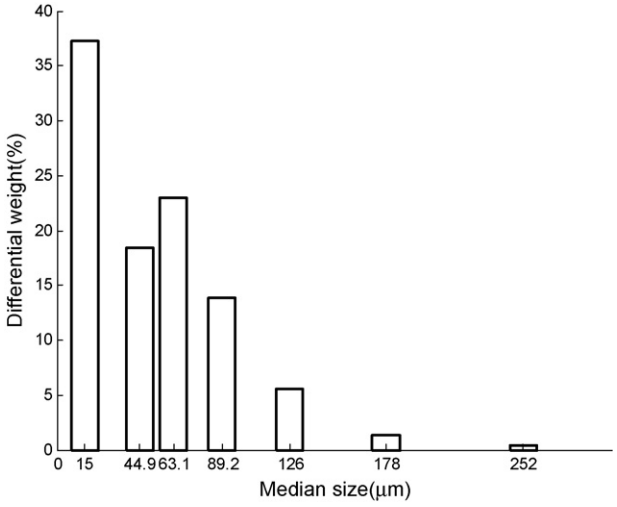

Fig. 4. Size distribution of Pittsburgh seam coal dust.

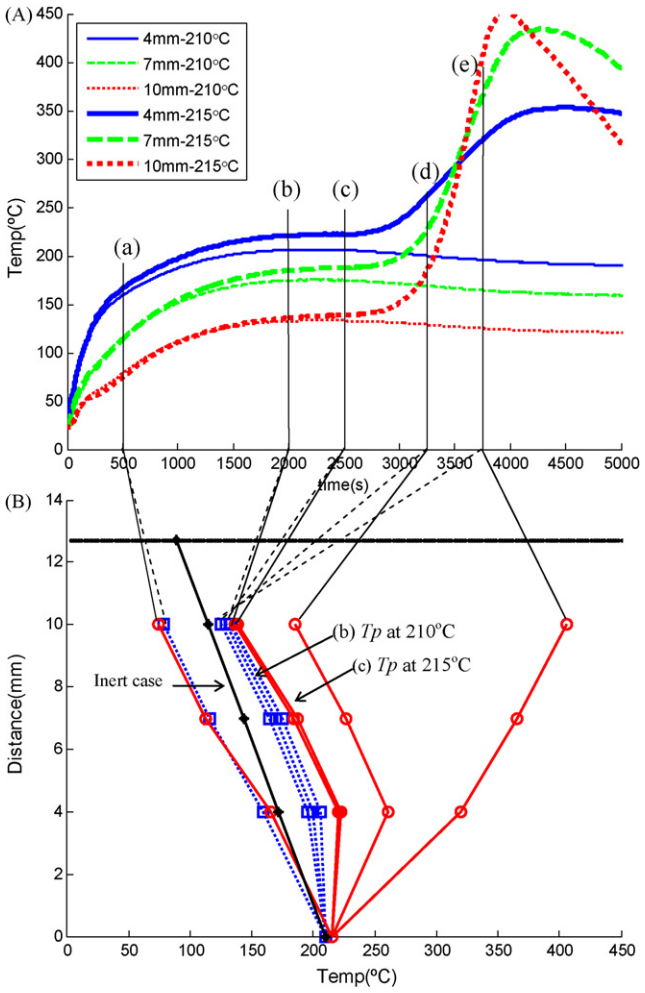

Fig. 5. Pittsburgh seam coal dust layer temperatures for a 12.7 mm layer thickness (A) and temperature distributions in the dust layer at corresponding times and inert consideration of coal dust layer (B). In (B), dotted connection line and square marker for T_p of 210 °C, solid connection line and round maker for T_p of 215 °C, and asterisk marker for inert case at T_p of 210 °C.

and e, respectively. Times were selected to highlight aspects of the thermal runaway theory discussed earlier (Fig. 1B). Line (a) represents a typical temperature in the transient period where heat flux from the hot plate increases the dust layer temperature with both a T_p value of 210 and 215 °C. Between (b) and (c), a transient temperature plateau is shown with a T_p value of 215 °C as is the result of T_p of 210 °C. Significant temperature rise during thermal runaway is observed over the period from line (c) to (e) with T_p of 215 °C as opposed to T_p of 210 °C with which temperatures slowly decrease and reach steady state.

The presumed temperature distribution in Fig. 1(B) shows good agreement with experimental results in Fig. 5(B). T_p of 215 °C at which thermal runaway is observed can be interpreted as T_{p4}, and T_p of 210 °C can be considered T_{p2} being located very near to T_{p3} in Fig. 1(B). Therefore, T_{p3}, the maximum hot surface temperature for steady state exists between 210 and 215 °C. Dust layer temperature with T_p of 210 °C at (e) in Fig. 5 can be considered point A in Fig. 1(A) where heat generation and loss rate are balanced. Temperature profile equivalent to the maximum steady state point B in Fig. 1(A) is not explicitly shown, but exists between (b) and (c) in Fig. 5(B). The maximum layer temperature with T_p of 210 °C is closest to the point B in Fig. 1(A).

Temperatures at all measured points in between (b) and (c) are higher than those of the inert case as shown in Fig. 5(B). This can be explained by the role of heat generation rate in the dust layer which the inert case does not take into account. The amount of temperature rise depends on the parameter values in the heat generation rate term. The non-dimensional heat generation rate term, δ in Eq. (3c), shows the associated parameters affecting the temperatures in the dust layer and the relationship of each parameter to one another.

Thermal runaway was observed at T_p of 250, 215, 200, and 190 °C for 6.4, 12.7, 19.1, and 25.4 mm thick Pittsburgh seam coal dust layers, respectively, as shown in Fig. 6. All temperature profiles in Fig. 6 were obtained from a single test. For 12.7 mm dust layer thickness when thermal runaway did not occur, the maximum dust layer temperature of 207 °C was recorded at 4 mm height, which is very close to T_p, but did not surpass it. The assumption for the Eq. (5), $d\theta/dz = 0$ at z = 0, is in agreement with this result. Time to reach steady state increased as the dust layer thickness increased.

Temperature crossover where the temperature of higher location in the dust layer exceeded those of lower locations was observed except for the 6.4 mm thick dust layer case. The temperature inversion may be caused by the higher oxygen diffusion near the surface facilitating more exothermic reaction in upper region of dust layer. However, oxygen concentration when thermal runaway does not occur is not a limiting factor of exothermic reaction rate [29]. Therefore, it does not have a significant effect on the steady state temperature profile in the dust layer and the following parameter estimation.

4. Parameter estimation

The hot surface ignition of a dust layer is a complex problem since factors such as particle size, contaminants, moisture, etc. are known to influence the minimum ignition temperature. Different contents and impurities of a coal can be roughly, but more often, summarized by a coal rank which also indicates the level of energy. However, it is reported that regardless of coal rank, critical temperature of coal particles with 0.06 mm diameter is about 400 K in oven-basket test [30], meaning that naturally inherent varying contents in coals may not play a critical role in thermal runaway phenomena. Therefore, in this study, Pittsburgh seam coal dust layer is assumed to be a homogenous material. A single 12.7 mm thick dust layer provides test results to estimate thermal conductivity, activation energy, and the coupled pre-exponential term. From multiple thermocouples buried in the dust layer, steady state temperature distribution of the dust layer is found. The parameters are estimated by comparing the experimentally obtained temperature distribution to the numerically predicted temperature distribution.

4.1. Estimation of thermal conductivity

Effective thermal conductivity of the dust layer can be estimated by assuming that heat generation at low temperature is negligible. Since the heat generation rate shows significant dependency on the local dust layer temperature, it may not be negligible near the critical temperature of thermal runaway. However, the assumption can be achieved if the hot plate temperature is sufficiently low.

(a) Neglecting heat generation term in Eq. (1) yields,

$$\frac{\partial^2 T}{\partial x^2} = 0 \tag{6}$$

(b) Integration of Eq. (6) with respect to the distance from the hot surface (x) leads to a constant value of dT/dx, which yields linear temperature profile in the dust layer. dT/dx is equal to the difference of Ts and T_p over the layer thickness.

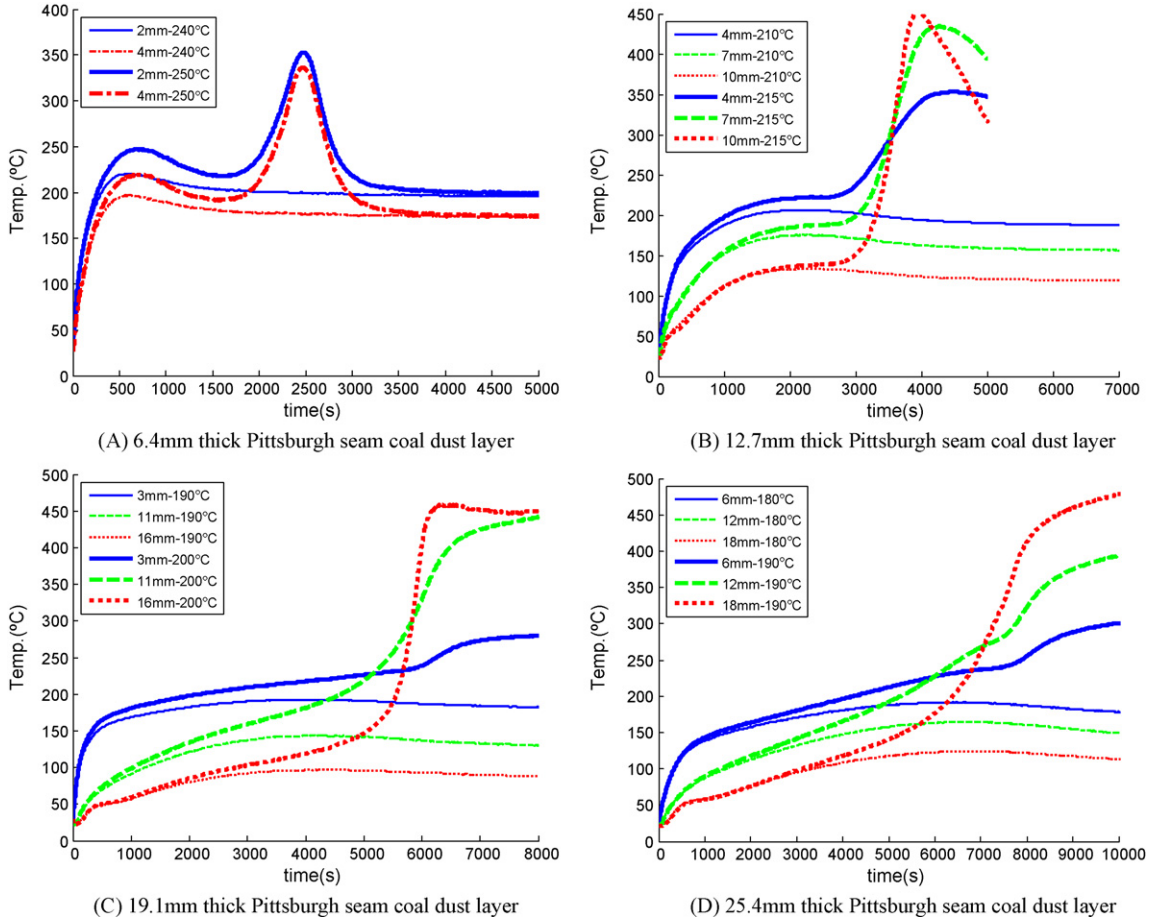

Fig. 6. Temperature profile vs. time for 6.4, 12.7, 19.1, and 25.4 mm thick Pittsburgh seam coal dust layer.

(c) From Eq. (2b), thermal conductivity can be written as,

$$k = -h_t(T_s - T_a)\frac{dx}{dT} = \frac{-h_t(T_s - T_a)dx}{(T_s - T_p)} \quad (7)$$

where dx = the thickness of the dust layer (0.0127 m).

(d) In Eq. (7), T_s can be obtained from the linear extrapolation of experimentally obtained steady state temperature profile of dust layer.

(e) In Eq. (7), effective total heat transfer coefficient, h_t, is comprised of convective heat transfer coefficient, h_c, and radiant heat transfer coefficient, h_r.

Convective heat transfer coefficient, h_c, is estimated from the correlation for natural convection of a horizontal plate with hot surface facing up [31,32].

$$h_c = \frac{0.54Ra^{0.25}k_a}{L}, \quad \text{for } 10^5 \approx< \text{Ra} \approx< 10^7 \quad (8)$$

where k_a = thermal conductivity of air (W/m K), L = characteristic length as the side of square having the same area of dust layer surface (m), $\text{Ra} = g\beta(T_s - T_a)L^3/\nu\alpha$, g = gravity (9.81 m/s^2), β = inverse film temperature (1/K), ν = kinematic viscosity of air (m^2/s), α = thermal diffusivity of air (m^2/s). T_a = ambient temperature (K). All the properties are estimated at the film temperature, the average value of the top surface temperature and ambient temperature.

Radiant heat transfer coefficient, h_r, is obtained by linearizing the radiant heat transfer at the surface as shown in Eq. (9).

$$\dot{q}'' = \varepsilon\sigma(T_s^4 - T_a^4) = h_r(T_s - T_a)$$
$$h_r = \varepsilon\sigma(T_s^2 + T_a^2)(T_s + T_a) \quad (9)$$

where ε = the coal emissivity (=0.9 [33]), and σ = Stefan–Boltzmann constant (5.67×10^{-8} W/m^2 K^4).

Temperatures measured at heights of 4, 7 and 10 mm in the 12.7 mm thick dust layer exposed to a hot surface temperature of 50 °C are shown in Fig. 7(A). Averaged temperatures from 1000 to 2500 s at each location are deemed to be steady state temperatures: 46, 41, and 37.4 °C for 4, 7, and 10 mm, respectively. Linear extrapolation from the three temperature yields T_s of 34.5 °C as shown in Fig. 7(B). h_c of 4.6 W/m^2 K is obtained with T_s = 34.5 °C, and $\text{Ra} = 7.55 \times 10^5$ which satisfies the condition for Eq. (8). In addition, k_a = 0.026 W/m K, and L = 0.09 m. The radiative heat transfer coefficient, h_r equals 5.6 W/m^2 K and is estimated with T_s = 34.5 °C. The total heat transfer coefficient, h_t = 10.2 W/m^2 K from the summation of h_c and h_r.

From Eq. (7), the estimated thermal conductivity is 0.1 W/m K with T_s of 34.5 °C and h_t of 10.2 W/m^2 K. The value of the thermal conductivity (0.1 W/m K) is the same as found by Reddy et al. [28] and Jones [10]. Thermal conductivity is assumed to be a constant value, i.e. not a function of temperature, and this is reasonable approximation for Pittsburgh seam coal dust. Negligible difference of thermal conductivity in the range of 50–250 °C was reported by Singer and Tye [26].

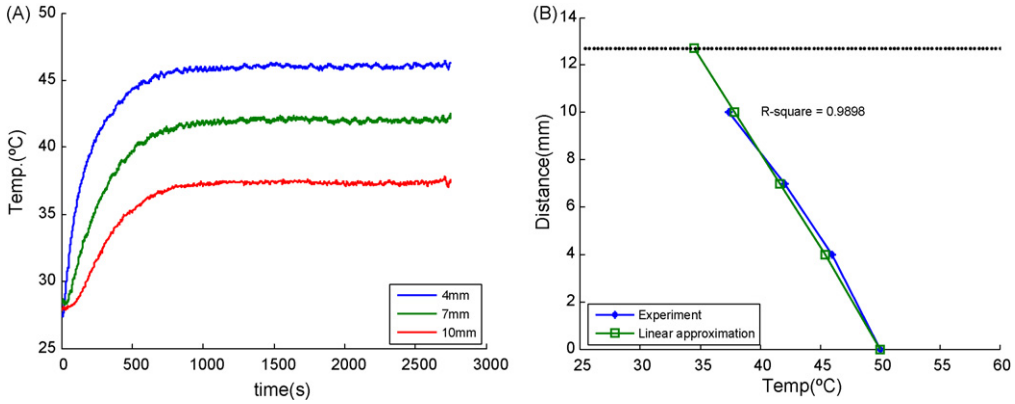

Fig. 7. 12.7 mm dust layer temperatures at different heights exposed to a hot surface of 50 °C (A), and steady state temperature distribution in the dust layer and its linear trend line (B).

4.2. Estimation of E and QA

Activation energy (E), and the coupled pre-exponential term (QA) are obtained from a single 12.7 mm thick dust layer experiment using a numerical optimization method. E and QA are estimated by comparing the two steady state dust layer temperature profiles which are, respectively, obtained from the experiment and from the numerical model. E, as an input parameter to the numerical model, is chosen from the best fitting case at which two temperature profiles show the least difference.

The numerical model for steady state temperature profile with the heat generation term being accounted for is developed. Discretization of Eq. (1) with the second order accuracy yields,

$$\frac{T_{i+1} - 2T_i + T_{i-1}}{\mathrm{d}x^2} = -\frac{\rho QA}{k} \mathrm{e}^{-E/RT_i} \tag{10}$$

Due to the non-linear term in the right hand side of Eq. (10), an iterative method is required to find converged values of temperature. 0.1 °C is used as the convergence criterion. The numerical model requires the values of unknown parameters, E and QA in the heat generation rate term, and the application of bottom and top boundary condition to be a numerically well-posed problem.

The values of E and QA are required, but neither value is known. Numerous combinations of E and QA which satisfy the experimental results of steady state at T_p of 210 °C and of thermal runaway at T_p of 215 °C are possible. However, a specific relationship between E and QA exists at the critical hot surface temperature. By correlating QA as a function of E, the numerical model can be completed with only one unknown parameter, E. The existence of the specific correlation between E and QA can be found from the fundamental steady state thermal runaway theory.

For a given E and T_p at which steady state temperature profile is obtained, as QA decreases, temperature distribution consequently becomes closer to the temperature distribution of an inert substance, which implies heat generation rate is an increasing function of QA. If QA increases, the dust layer temperature increases, but only up to a specific value beyond which heat generation rate term becomes too large for steady state dust layer temperature. Therefore, at critical hot surface temperature where the maximum heat generation rate for steady state is recorded, the value of QA becomes also the maximum for a given E.

The procedure to obtain a correlation between E and QA is given below:

(a) The critical non-dimensional heat generation rate term, δ_c, is derived by substituting T_p with T_{p3} in Eq. (3c). Taking the logarithm of both sides of δ_c yields,

$$\ln(QA) = \frac{1}{RT_{p3}} E + \ln\left(\frac{\delta_c R T_{p3}^2 k}{Er^2 \rho}\right). \tag{11}$$

A correlation that satisfies Eq. (11) for various pairs of E and δ_c values can be obtained by interpolating the various points of $\ln(QA)$ vs. E.

(b) In Eq. (11), T_{p3} and δ_c are required to calculate the value of $\ln(QA)$ for a given E. For Pittsburgh seam coal used in this study, T_{p3} ranges from 210 to 215 °C at a layer thickness of 12.7 mm. δ_c is calculated from Eq. (5) in which Bi and θ_a are required. Bi is calculated from Eq. (12) derived by substituting k with Eq. (7) from its definition [19],

$$Bi = \frac{h_t r}{k} = \frac{T_p - T_s}{2(T_s - T_a)} \tag{12}$$

In Eq. (12), T_s is calculated assuming the dust layer as an inert material which yields the linear temperature profile in the dust layer [19]. In Eq. (7), with k as 0.1 W/m K, the unknown parameters are T_s and h_t. Since T_s is required for the calculation of h_t consisting of h_c and h_r, T_s is initially assumed and updated iteratively to satisfy both Eq. (7) and h_t. θ_a is obtained from Eq. (3b) with the given E. Since the correlation between $\ln(QA)$ and E is sought at the criticality, T_p is replaced by T_{p3} in the calculation of Bi and θ_a. Considering 210 and 215 °C as two bounding values of T_{p3}, two $\ln(QA)$ and E correlations are obtained.

(c) All the parameters required for $\ln(QA)$ are calculated in step (b) for a given E. Now, by varying E within the expected range, the value of $\ln(QA)$ can be obtained for the corresponding E. The $\ln(QA)$ and E correlation is obtained by interpolating various points of $\ln(QA)$ vs. E.

An initial value of E needed for the calculation of δ_c in step (b), is obtained from Table 1, where values of E range between 40 to 120 kJ/mol. Taking E of 120 kJ/mol and T_{p3} of 210 °C as a sample case, δ_c of 8.78 is calculated using Eq. (5) with θ_a as −11.6 and Bi as 0.9. T_s of 89 °C and h_t of 14.2 W/m^2 K are calculated. $\ln(QA)$ of 36.4 is calculated for E of 120 kJ/mol.

For the same E, with T_{p3} of 215 °C which yields T_s of 90.4 °C and h_t of 14.3 W/m^2 K, $\ln(QA)$ becomes 36.1 with δ_c of 8.93. θ_a of −11.7 and Bi of 0.9 are calculated. Two values of $\ln(QA)$ are derived from Eq. (11) for 120 kJ/mol: 36.4 with T_{p3} of 210 °C and 36.1 with T_{p3} of 215 °C.

In the same way, decreasing E to 40 kJ/mol, corresponding values of QA can be obtained for each T_{p3}. Interpolating various points of $\ln(QA)$ and E, two linear correlations with R-square of unity are obtained as shown in Fig. 8(A): $\ln(QA) = 2.5777 \times 10^{-4} E + 5.4685$

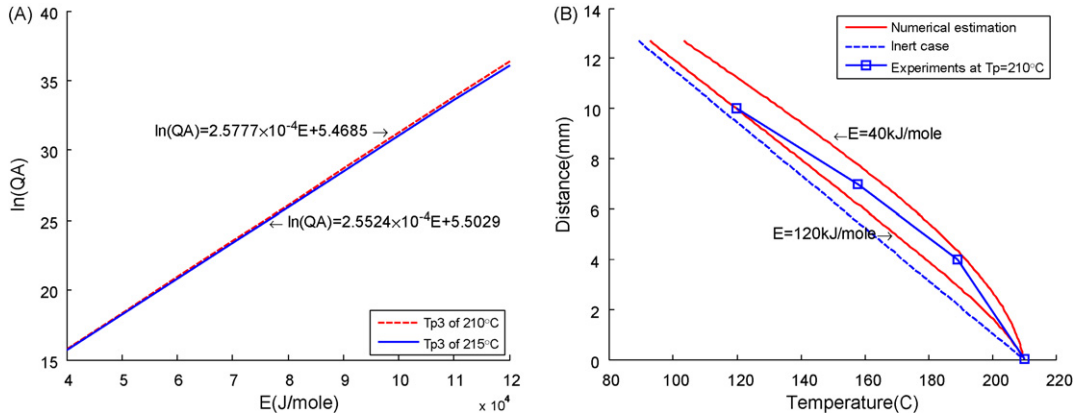

Fig. 8. Pairs of E and ln(QA) with T_p of 210 and 215 °C (A) and numerical estimation at T_p of 210 °C with E = 40 and 120 kJ/mol and corresponding QAs obtained from the correlation with T_{p3} of 215 °C (B).

with T_{p3} of 210 °C, and ln(QA) = 2.5524 × $10^{-4}E$ + 5.5029 with T_{p3} of 215 °C. Nugroho et al. [30] also reported linear relationship between ln(QA) and E at criticality for various coal types.

Now, QA in the heat generation rate term in Eq. (10) can be replaced by a function of E which leaves E as the only unknown parameter such that experimental results can be compared to the numerical results by changing only E. It also provides the lower and upper bounding values of QA for a given E which satisfies the experimental fact that the maximum hot surface temperature for steady state lies between 210 and 215 °C.

Lower and upper surface boundary conditions need to be applied to fulfill the well-posed problem. The lower surface boundary condition of Eq. (2a) is applied to the model as an input value. The upper surface boundary condition of Eq. (2b) requires k, T_s, and h_t. T_s and h_t can be obtained from Eq. (7) as can be in the calculation for the ln(QA) and E correlations if T_p is known. Therefore, the top boundary condition is defined by the bottom boundary condition, which leaves T_p as the only input value in terms of the application of boundary conditions to the numerical model.

The numerical model for steady state dust layer temperature profile is completed with the input values of T_p and E. By varying E, the steady state dust layer temperature profile obtained from the numerical model can be compared to the experimentally obtained temperature profile at the same T_p. T_p can be any value as long as steady state temperature distribution is obtained, but the effect of E and QA is the most distinctive on the dust layer temperature profile, if T_p is closer to the T_{p3}. Since the steady state temperature distribution at 210 °C is available from the experiment, and in the range of T_{p3}, T_p of 210 °C is used for comparison.

Average dust layer temperatures from 5000 to 7000 s at 4, 7, and 10 mm heights are used as steady state temperatures: 188.6 °C at 4 mm, 157.5 °C at 7 mm, and 119.6 °C at 10 mm as can be seen in Fig. 6(B). This experimentally obtained temperature distribution of 12.7 mm thick dust layer is compared to the numerically estimated temperature distributions with two bounding values of E, 40 and 120 kJ/mol as found in Table 1, and with the ln(QA) and E correlation derived from T_{p3} at 215 °C in Fig. 8(B). T_{p3} of 215 °C is not the actual hot surface temperature to which dust layer is exposed, but the temperature used to obtain the ln(QA) and E correlation. Less temperature rise in the dust layer is found with higher activation energy in the numerical model. Considering activation energy as thermal barrier for exothermic reaction to occur, less heat is generated in the dust layer with higher activation energy for the same T_p such that less temperature rise is reasonable. Reasonable temperature distributions are estimated from the numerical model based on the bounding values of E as shown in Fig. 8(B).

The sums of absolute values of temperature differences at 4, 7, and 10 mm locations between numerical estimation and experimental data at various activation energies are shown in Fig. 9(A). The best fitting curve of the numerical model to the experiment yields two optimized values of E (and QA) from each ln(QA) and E correlation: one based on T_{p3} of 210 °C and the other one based on T_{p3} of 215 °C, specifically considering the steady state temperature of 12.7 mm thick dust layer exposed to T_p of 210 °C. With the least temperature difference between numerical model and experimental data at 4, 7, and 10 mm as a criterion, E of 83.1 kJ/mol (QA of 4.8 × 10^{11} J/kg s), and E of 61.7 kJ/mol (QA of 1.7 × 10^9 J/kg s) are obtained

Numerically estimated temperature profiles with the obtained best fitting values of E (and QA) are plotted in Fig. 9(B) showing relatively good agreement with the experimental data except for the 10 mm height. This may be due to the higher convective and radiant heat loss near the top surface in actual conditions. Since the dust layer surface is composed of particles, and thus, the real surface area on which the amount of convective and radiant heat loss depends is larger than the theoretical model for numerical estimation.

4.3. Estimation of T_{p3} for other thicknesses

From section 4.2, E and QA are estimated from a single 12.7 mm thick dust layer with multiple thermocouples in it. E is expected to range from 61.7 to 83.1 kJ/mol with QA of 1.7 × 10^9 and 4.8 × 10^{11} J/kg s, correspondingly. The estimated E and QA values are used to predict the critical hot surface temperatures (T_{p3}) for the other thicknesses: 6.4, 19.1, and 25.4 mm. The estimation of T_{p3} for a given dust layer thickness is practically useful, since in reality, dust layer thickness is measurable, and thus, the maximum safe hot surface temperature for thermal runaway often needs to be known. In this section, the predicted T_{p3} for each thickness is compared to the experimentally obtained T_{p3} for the purpose of validation of the current numerical estimation method of E and QA. The values of E and QA are also compared to the values obtained from widely known multiple tests method. Detailed calculations of multiple tests method are included in Appendix A.

T_{p3} is obtained from the case that δ from Eq. (3c) with T_p replaced by T_{p3} becomes the same with δ_c from Eq. (5). Since Bi in Eq. (5) includes a dependent variable, T_s, which is determined from T_{p3} with the assumption of the dust layer being an inert material, T_{p3} should be initially assumed and improved iteratively until it satisfies both values of δ_c from Eqs. (3c) and (5). Calculation step for T_s is the same with step (b) in Section 4.2.

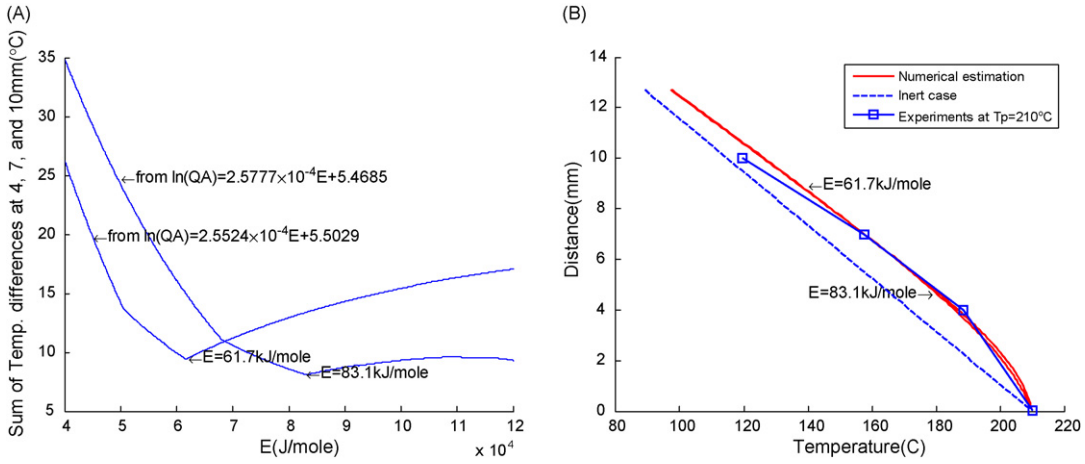

Fig. 9. Sum of the absolute values of temperature differences between numerical estimation and experimental data in 4, 7, and 10 mm heights at various activation energies (A) and numerically estimated dust layer temperature distribution with obtained E: 61.7 and 83.1 kJ/mol (B).

Since the values of E and QA are not a specific single value, but a range, mean values of E and QA are selected for the prediction of T_{p3} of the other thicknesses: 6.4, 19.1, and 25.4 mm. To check the prediction uncertainty of the numerical model, two bounding pairs of values of E and QA are also used. E of 72.4 kJ/mol is calculated as the mean value, and QA of 2.8×10^{10} J/kg s is obtained by averaging the values of ln(QA) from the two ln(QA) and E correlations with E of 72.4 kJ/mol. The mean values of E and QA correspond to the case that T_{p3} is assumed to be the mean value of 210 and 215 °C for 12.7 mm thick dust layer. Two bounding pairs of E and QA were estimated from the fact that T_{p3} lies between 210 and 215 °C for 12.7 mm thick dust layer. The associated parameter values and calculated T_{p3} values with the three pairs of E and QA are shown in Table 2. Relative deviations of estimated T_{p3} for each thickness and for each pair of E and QA are shown in Fig. 10 in comparison with the experimental values. Since T_{p3} has a 10 °C error range based on the test resolution of T_p in the experiment, if the predicted T_{p3} for the other thicknesses are located in the gray box area in Fig. 10, the current estimation procedure of E and QA can be considered reasonable, and if not, the magnitude of the deviation implies the error range of the current method.

For the mean values of E and QA, the predicted T_{p3} for the other thicknesses are located in the experimental range (gray box) which indicates that the use of mean values of E and QA are reasonable. An additional implication is that the real T_{p3} for 12.7 mm thick dust layer is closer to 212.5 °C. For the bounding pairs of values of E and QA, the predicted T_{p3} for 19.1 mm thick dust layer falls within the experimental range, however for 6.4 mm and 25.4 mm thick dust layers, predicted T_{p3} values fall outside of the experimental range by a maximum of 5.4 and 3.8 °C, respectively. The deviation may be caused by various approximations used for the calculations such as the dust layer being an inert material which yields lower T_s than the actual and subsequent error of Bi, and the approximate solution of δ_c of Eq. (5). However, considering that the amount of deviation is not much larger than the experimental error range and that the mean value of E and QA predicts T_{p3} within the range, the numerical method to estimate E and QA is considered to be stable and reasonable. The deviation can be decreased by finding more narrow range of T_{p3} for 12.7 mm thick dust layer from which the ln(QA) and E correlations are derived.

Table 2
Estimated T_{p3} and associated parameter values for the other thicknesses: 6.4, 19.1, and 25.4 mm from the mean and bounding values of E and QA.

E (kJ/mol)	QA (J/kg s)	$2r$ (mm)	T_s (°C)	Bi	θ_a	δ_c	T_{p3} (°C)
72.4	2.8×10^{10}	6.4	130.6	0.5	−7.2	2.5	245.2
		19.1	71.1	1.3	−6.9	4.4	194.2
		25.4	60.2	1.6	−6.7	4.7	180.8
61.7	1.7×10^{9}	6.4	134.7	0.5	−6.2	1.9	255.4
		19.1	70.6	1.3	−5.8	3.3	192.2
		25.4	59.2	1.6	−5.7	3.6	176.2
83.1	4.8×10^{11}	6.4	127.1	0.5	−8.3	3.0	236.8
		19.1	71.1	1.3	−7.9	5.5	194.4
		25.4	60.6	1.6	−7.7	6.0	183.0

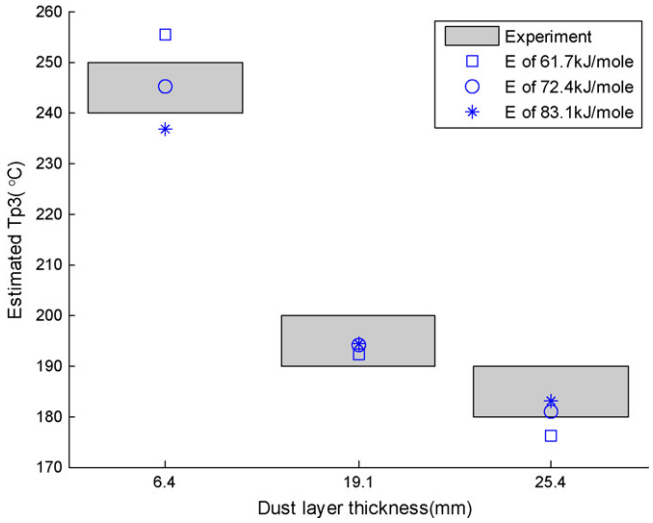

Fig. 10. Estimated T_{p3} for each thickness and deviation of E as compared to the experiment.

5. Conclusion

Whether or not a hot surface temperature is sufficiently high to cause thermal runaway is determined by the comparison of the non-dimensional heat generation rate (δ) with the critical heat generation rate (δ_c). If δ is less than δ_c, meaning heat generation rate at the current hot surface temperature is less than the critical temperature, thermal runaway is not expected to occur. For this comparison, not only are measurable physical properties, such as density, ambient temperature, and thickness of dust layer, required, but also thermal and kinetic parameters, including thermal conductivity (k), activation energy (E), and coupled pre-exponential term (QA) need to be known.

Table 3
The minimum and maximum values of activation energy (E) and the corresponding coupled pre-exponential term (QA) with the combination of LITs.

Layer thickness (mm)	6.4	19.1	25.4	E (kJ/mol)	QA (J/kg s)
The possible maximum steady state hot surface temperature (T_{p3}) (°C)	250 240	190 200	180 190	66.8 89.1	6.6×10^9 1.8×10^{12}

Exploring thermal runaway theory, hot surface ignition tests have been conducted with four different dust layer thicknesses: 6.4, 12.7, 19.1 and 25.4 mm using Pittsburgh seam coal dust and a slightly modified standard ASTM E 2021 test apparatus. The ranges of the maximum hot surface temperature (T_{p3}) for the dust layer to remain in steady state were found for each thickness. Multiple thermocouples were located in the dust layer such that the steady state temperature distribution was determined at a given hot surface temperature.

k, E and QA were obtained from a single 12.7 mm thick dust layer with a numerical optimization method. k of 0.1 W/m K was estimated assuming negligible heat generation at the hot surface temperature of 50 °C, and matched the previously reported literature value [10,25]. To estimate E and QA, the multiple tests method requires different hot plate temperatures, and thus, different thicknesses of dust layer are needed to be tested. Instead of multiple hot surface temperatures, multiple thermocouples enabled the comparison of steady state dust layer temperature profiles obtained from a numerical optimization method and the experiment to be used to estimate E and QA. E of 61.7 to 83.1 kJ/mol and QA of 1.7×10^9–4.8×10^{11} J/kg s were obtained from a single 12.7 mm thick dust layer. The estimated E and QA were then used to predict the critical hot surface temperatures of the other thicknesses: 6.4, 19.1, and 25.4 mm for validation purpose. From the experiment, the critical hot surface temperatures for 6.4, 19.1, and 25.4 mm thick dust layer ranged between 240 and 250 °C, 190 and 200 °C, and 180 and 190 °C, respectively, with 10 °C experimental error range. The mean values of E and QA, E of 72.4 kJ/mol and QA of 2.8×10^{10} J/kg s, predicted the critical hot surface temperatures for the other thicknesses within the experimental error range and the maximum deviation outside the experimental error range of 6 °C was observed with two bounding values of E and QA, E of 61.7 kJ/mol (and QA of 1.7×10^9 J/kg s) and 83.1 kJ/mol (and QA of 4.8×10^{11} J/kg s), which shows the presented numerical optimization method to estimate E and QA to be reasonable. The estimated E and QA values also matched well with the values obtained from widely accepted multiple tests method (E of 66.8–89.1 kJ/mol and QA of 6.6×10^9–1.8×10^{12} J/kg s) as described in Appendix A. The current estimation method with Pittsburgh seam coal shows satisfactory results as it applies to different dust layer thicknesses, and as compared to the multiple tests method. Further research must address broader applications of this method for different coal types.

Acknowledgements

The authors thank Dr. K.L. Cashdollar, I.A. Zlowchower, and A.C. Smith in NIOSH Pittsburgh research laboratory for providing Pittsburgh seam coal and valuable references, Dr. T. Myers in Exponent, Inc. for allowing use of stainless steel rings, and R.K. Harris in WPI fire laboratory for experimental support.

Appendix A

Logarithm of the critical non-dimensional heat generation rate term, δ_c, from Eq. (3c) substituting T_p with T_{p3}, yields,

$$\ln\left(\frac{\delta_c T_{p3}^2}{r^2}\right) = -\frac{E}{RT_{p3}} + \ln\left(\frac{E}{R}\frac{\rho QA}{k}\right) \quad (13)$$

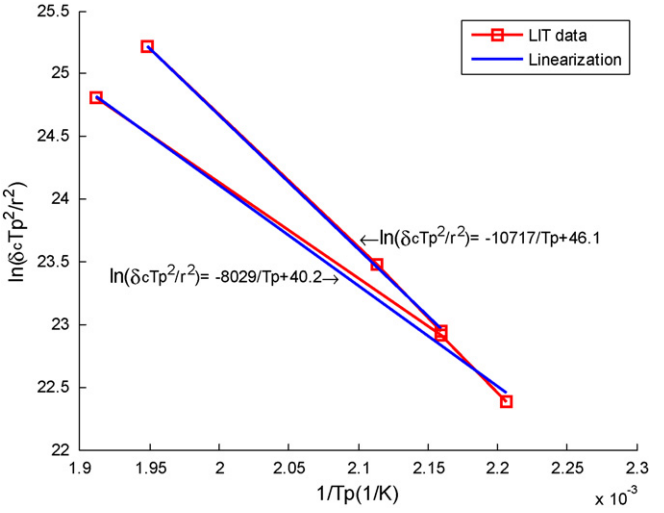

Fig. 11. Possible layer ignition temperatures (LITs) data of Pittsburgh seam coal dust layer to obtain E and QA.

Activation energy (E) is obtained from the slope of the linearized interpolation line of the multiple points of $\ln(\delta_c T_{p3}^2/r^2)$ vs. $1/T_{p3}$. Several different T_{p3} values which can be obtained from the experiments with different dust layer thicknesses are required for plotting multiple points. With this method, Reddy et al. [28] reported E and QA of Pittsburgh seam coal dust as shown in Table 1 based on the results of Mirron and Lazzara's tests [8].

To have an independent check of E numerically estimated from 12.7 mm thick dust layer, test results from 6.4, 19.1, and 25.4 mm thickness are used for the calculation of multiple tests method. LITs of 250, 200, and 190 °C were obtained for 6.4, 19.1, and 25.4 mm thick Pittsburgh coal dust layer, and thermal runaway was not observed at 240, 190, and 180 °C for each thickness. Due to the relatively large test resolution of hot surface temperature which is 10 °C, T_{p3} for each thickness can be any temperature between the two boundary temperatures. For example, any temperature greater than or equal to 240 °C and less than 250 °C can be T_{p3} of 6.4 mm thick layer, and consequently, the set of T_{p3} of each thickness can vary as much leading to different value of E. Jones et al. [34] also mentioned the error in E estimation is mainly caused by the uncertainty of T_{p3}.

From reviewing all the possible cases of T_{p3} for each thickness, the combinations of T_{p3} resulting in the minimum and maximum values of E and corresponding QA's are shown in Table 3. As shown in Table 3, 250 °C is used as T_{p3} for 6.4 mm thickness at which thermal runaway was observed. However, adopting infinitesimally small test resolution, the possible T_{p3} for steady state can become 250 °C with negligible error. Estimated E ranges from 66.8 to 89.1 kJ/mol. Fig. 11 shows relative relationship of the two data sets from which the minimum and maximum value of E results.

Table 4
E and QA from numerical estimation and multiple tests method.

	Numerical estimation	Multiple tests method
E (kJ/mol)	61.7–83.1	66.8–89.1
QA (J/kg s)	1.7×10^9–4.8×10^{11}	6.6×10^9–1.8×10^{12}

Table 4 shows activation energy and pre-exponential term obtained from numerical estimation and the multiple tests method. E from numerical estimation is slight less than multiple tests method, but shows good agreement.

References

[1] V. Fierro, J.L. Miranda, C. Romero, J.M. Andres, A. Arriaga, D. Schmal, Model predictions and experimental results on self-heating prevention of stockpiled coals, Fuel 80 (2001) 125–134.
[2] M.A. Smith, D. Glasser, Spontaneous combustion of carbonaceous stockpiles. Part II. Factors affecting the rate of the low-temperature oxidation reaction, Fuel 84 (2005) 1161–1170.
[3] U. Krause, M. Schmidt, C. Loher, A numerical model to simulate smouldering fires in bulk materials and dust deposits, Journal of Loss Prevention in the Process Industries 19 (2006) 218–226.
[4] D.N. Galushkin, N.N. Yazvinskaya, N.E. Galushkin, Investigation of the process of thermal runaway in nickel-cadmium accumulators, Journal of Power Sources 177 (2008) 610–616.
[5] Z. Dyduch, B. Majcher, Ignition of a dust layer by a constant heat flux-heat transport in the layer, Journal of Loss Prevention 19 (2006) 233–237.
[6] H.J. Park, Hot surface ignition temperature of dust layers with and without combustible additives. MS thesis:WPI (2006).
[7] V. Babrauskas, Ignition Handbook, Fire Science Publishers, Washington, 2003.
[8] Y. Mirron, C.P. Lazzara, Hot-surface ignition temperatures of dust layers, Fire and Materials 12 (1988) 115–126.
[9] A.S. Rangwala, T.J. Myers, A.F. Ibarreta, Measurement of the non-dimensional frank-kamenetskii number using a standard dust layer ignition testing apparatus, in: 5th International Seminar on Fire and Explosion Hazards, University of Edinburgh, Edinburgh, UK, 2007.
[10] J.C. Jones, A new and more reliable test for the propensity of coals and carbons to spontaneous heating, Journal of Loss Prevention in the Process Industries 13 (2000) 69–71.
[11] J.C. Jones, Recent developments and improvements in test methods for propensity towards spontaneous heating, Fire and Materials 23 (1999) 239–243.
[12] L.P. Wiktorsson, W. Wanzl, Kinetic parameters for coal pyrolysis at low and high heating rates – a comparison of data from different laboratory equipment, Fuel 79 (2000) 701–716.
[13] ASTM E2021, Standard test method for hot surface ignition temperature of dust layers. ASTM 2003.
[14] N.N. Semenov, Chemical Kinetics and Chain Reactions, The Clarendon Press, Oxford, 1935.
[15] D.A. Frank-Kamenetskii, Diffusion and Heat Transfer in Chemical Kinetics, 2nd ed., Plenum Press, New York and London, 1969.
[16] P. Gray, P.R. Lee, Thermal Explosion Theory, Oxidation and Combustion Reviews, Elsevier, 1967, 1–183.
[17] P.C. Bowes, Self-Heating: Evaluating and Controlling the Hazards, Elsevier, London, 1984.
[18] P.H. Thomas, P.C. Bowes, Thermal ignition in a slab with one face at a constant high temperature, Transactions of the Faraday Society 57 (1961) 2007–2017.
[19] P.C. Bowes, S.E. Townshend, Ignition of combustible dusts on hot surfaces, British Journal of Applied Physics 13 (1962) 103–114.
[20] A. Rosema, H. Guan, H. Veld, Simulation of spontaneous combustion, to study the causes of coal fires in the Rujigou basin, Fuel 80 (2001) 7–16.
[21] J.B. Howard, R.H. Essenhigh, Pyrolysis of coal particles in pulverized fuel flames, Industrial & Engineering Chemistry Process Design and Development 6 (1967) 74–84.
[22] H.N. Stone, J.D. Batchelor, H.F. Johnstone, Low temperature carbonization rates in a fluidized bed, Industrial & Engineering Chemistry Process Design and Development 46 (1954) 274–278.
[23] T.N. Anthony, J.B. Howard, H.C. Hottel, H.P. Meissner, Rapid devolatilization of pulverized coal, in: 15th Symposium (International) on Combustion, 1975, pp. 1303–1317.
[24] H. Kobayashi, J.B. Howard, A.F. Sarofim, Coal devolatilization at high temperatures, in: 16th Symposium (International) on Combustion, 1977, pp. 411–415.
[25] L. Yuan, A. Smith, Computational fluid dynamics modeling of spontaneous heating in longwall gob areas, in: SME Annual Meeting, 2007.
[26] J.M. Singer, R.P. Tye, Thermal, mechanical, and physical properties of selected bituminous coals and cokes. Bureau of Mines Report RI 8364, 1979.
[27] J.M. Herrin, D. Deming, Thermal conductivity of U.S. coals, Journal of Geophysical Research 101 (1996) 25381–25386.
[28] P.D. Reddy, P.R. Amyotte, M.J. Pegg, Effect of inerts on layer ignition temperatures of coal dust, Combustion and Flame 114 (1988) 41–53.
[29] H.J. Park, R. Zalosh, Air flow and oxygen concentration effects in dust layer hot surface ignition temperature tests, in: 5th International Seminar on Fire and Explosion Hazards, University of Edinburgh, Edinburgh, UK, 2007.
[30] Y.S. Nugroho, A.C. Mcintosh, B.M. Gibbs, On the prediction of thermal runaway of coal piles of differing dimension by using a correlation between heat release and activation energy, in: Proceedings of the Combustion Institute, 28, 2000, pp. 2321–2327.
[31] M.T. Gratkowski, N.A. Dembsey, C.L. Beyler, Radiant smoldering ignition of plywood, Fire Safety Journal 41 (2006) 427–443.
[32] H.M. Kim, C.C. Hwang, Heating and ignition of combustible dust layers on a hot surface: influence of layer shrinkage, Combustion and Flame 105 (1996) 471–485.
[33] J. Adanez, F.G. Labiano, Modeling of moving-bed coal gasifiers, Industrial and Engineering Chemistry 29 (1990) 2079–2088.
[34] J.C. Jones, P.S. Chiz, R. Koh, J. Matthew, Kinetic parameters of oxidation of bituminous coals from heat-release rate measurements, Fuel 75 (1996) 1755–1757.